

Amelioration of bleomycin induced pulmonary fibrosis by administration of Salvianolic acid B in mice

Gulzar Begum¹, Nittin Dev Singh^{1*}, Geeta Devi Leishangthem² and Harmanjit Singh Banga¹

¹Department of Veterinary Pathology, College of Veterinary Science, Guru Angad Dev Veterinary and Animal Sciences University, Ludhiana, Punjab-141004, India.

²Animal Disease Research Centre, College of Veterinary Science, Guru Angad Dev Veterinary and Animal Sciences University, Ludhiana, Punjab-141004, India.

*Corresponding author at: Department of Veterinary Pathology, College of Veterinary Science, Guru Angad Dev Veterinary and Animal Sciences University, Ludhiana, Punjab-141004, India.
E-mail: drndsingh@gmail.com.

Veterinaria Italiana 2021, **58** (1), 87-101. doi: 10.12834/VetIt.1703.9039.2
Accepted: 31.08.2021 | Available on line: 16.11.2021

Keywords

Bleomycin,
Epithelial-mesenchymal transition,
Mice model,
Pulmonary fibrosis,
Salvianolic acid B.

Summary

Pulmonary fibrosis is the end-stage manifestation of wide range of respiratory diseases and during pulmonary fibrosis, pulmonary inflammation and epithelial-mesenchymal transition (EMT) play important roles. Salvianolic acid B (SAB) from the herb *Salviae miltiorrhiza* has been reported to possess an excellent anti-inflammatory, antifibrotic and antioxidant activity. The present study aimed to investigate the ameliorative effect of SAB on bleomycin induced pulmonary fibrosis in mice. Adult albino mice were divided as SHAM/control group (saline alone), BLM group (bleomycin @ 1mg/kg intratracheally once) and SAB groups (BLM challenged once and SAB administration in three dosages @ 5, 10 and 15 mg/kg intraperitoneally daily for 30 days). Lungs wet/dry ratio and protein concentration in bronchoalveolar lavage fluid, MPO activity, oxidative stress markers, hydroxyproline assay, levels of inflammatory cytokines (TNF- α , IL-6 and TGF- β 1), NF- κ B activity, histopathology, immunostaining (E-cadherin, vimentin and alpha-smooth muscle actin) and ultrastructural changes were studied. SAB showed anti-inflammatory and anti-fibrotic effects through inhibition of inflammatory cell infiltration, alveolar structure disruption, and collagen deposition and the expression of several fibrogenic cytokines. SAB also up-regulate E-cadherin and down-regulated vimentin and alpha-smooth muscle actin expression. In conclusion, Salvianolic acid B is effective in alleviating the BLM induced lung fibrosis through suppression of oxidative stress, inflammation, histological, ultrastructural changes and EMT.

Introduction

Pulmonary fibrosis, the end-stage manifestation of a wide range of respiratory diseases, is characterized by alveolar epithelial injury, initiation of inflammatory cascades, exaggerated profibrotic cytokine expression, increased extracellular matrix (ECM) deposition in the interstitium and parenchyma, which in the end lead to fibrotic lesion formation, respiratory failure and swift death. Epithelial-mesenchymal transition (EMT) which is a process in which epithelial cells gradually acquire a mesenchymal (fibroblast-like) cell phenotype, has been shown to play a pivot role in pulmonary fibrosis where cells like resident pulmonary fibroblasts or blood-borne fibrocytes, alveolar epithelial cells (AECs) undergo transdifferentiation and turn into myofibroblasts (Willis and Borok 2007). The EMT

process has been associated with lung fibrosis by acquiring the phenotype of myofibroblasts differentiated from epithelial cells (Chen *et al.* 2015).

Furthermore, pulmonary fibrosis denotes a major challenge and there are no effective cures for fibrosis, emphasizing that the lack of effective treatment signifies an unmet clinical need (Rosenbloom *et al.* 2017). It has been stated that the future therapeutic approach may focus on improvement in regeneration of alveolar epithelial cells (Rafi *et al.* 2013) and reversal of the process of EMT (Kagalwalla *et al.* 2012). Bleomycin (BLM) is an antibiotic agent isolated from the fungus *Streptomyces verticillus* and has been used as anti-cancer drug but it can cause, as side effect, lung toxicity leading to pulmonary fibrosis. BLM has been widely used in animals model (mice, rats and hamster) to study the mechanisms involved in fibrogenesis and to evaluate potential therapies

(Moeller *et al.* 2008). The standard and most common route of administration is the single intratracheal instillation of BLM which produces lung injury and resultant fibrosis in rodents (Borzzone *et al.* 2001).

Salvianolic acid B (SAB), water-soluble polyphenolic compound extracted from dried roots of a herb *Salvia miltiorrhiza*, is widely used in traditional Chinese medicine, often in combination with other herbs, to treat a diversity of ailments like cardio-vascular disease, hyperlipidemia and cerebro-vascular disease throughout the world (Cheng *et al.* 2007).

Few studies are available on attenuation of bleomycin induced pulmonary fibrosis using Salvianolic acid B (Liu *et al.* 2016). Therefore, the present study aimed to investigate the ameliorative effect of SAB on bleomycin-induced pulmonary fibrosis in mice.

Materials and methods

Animals and treatments

The study protocol was approved by the Institutional Animal Ethics Committee (IAEC) of Guru Angad Dev Veterinary and Animal Sciences University (GADVASU), Ludhiana. Male albino mice (n = 30, 4-6 weeks of age), were obtained from Disease free small animal house, Central Research Institute, Kasauli, Himachal Pradesh and housed in the small animal house of Gadvasu. After the acclimatization period of 7 days, the animals were weighed again and, 30 mice were randomly divided into five experimental groups (6 animals each) and

named as per the challenge and treatment: SHAM/PBS (saline-only/control group), BLM (bleomycin @ 1 mg/kg group), BLM/SAB/5 (bleomycin/salvianolic acid B @ 5mg/kg), BLM/SAB/10 (bleomycin/salvianolic acid B @ 10mg/kg) and BLM/SAB/15 (bleomycin/salvianolic acid B @ 15 mg/kg). Mice received a single intratracheal instillation of saline containing bleomycin sulfate @ 1 mg/kg bw (Sigma, USA) in a volume of 50 μ l in all groups, except vehicle group. Salvianolic acid B (Sigma, USA) in three different dosages (5, 10 and 15 mg/kg) was given intraperitoneally daily for 1 month. All the mice were sacrificed after 1 month by ketamine and xylazine overdose (Figure 1A).

Collection of bronchoalveolar lavage fluid (BALF)

Bronchoalveolar lavage was performed through a tracheal cannula attached to 1 ml syringe with 0.5 mL of PBS in each animal from the left lung. Bronchoalveolar lavage fluid was processed to get cell pellets and supernatants as described earlier (Mabalarajan *et al.* 2010). Total cell and differential counts were performed with resultant cell pellets using a haemocytometer and staining with Leishman stain. BALF supernatant was collected and stored at - 80 °C for estimation of protein concentration, TNF- α and IL-6.

Wet to dry lung weight ratio

After sacrificing the animals, similar lobe of right

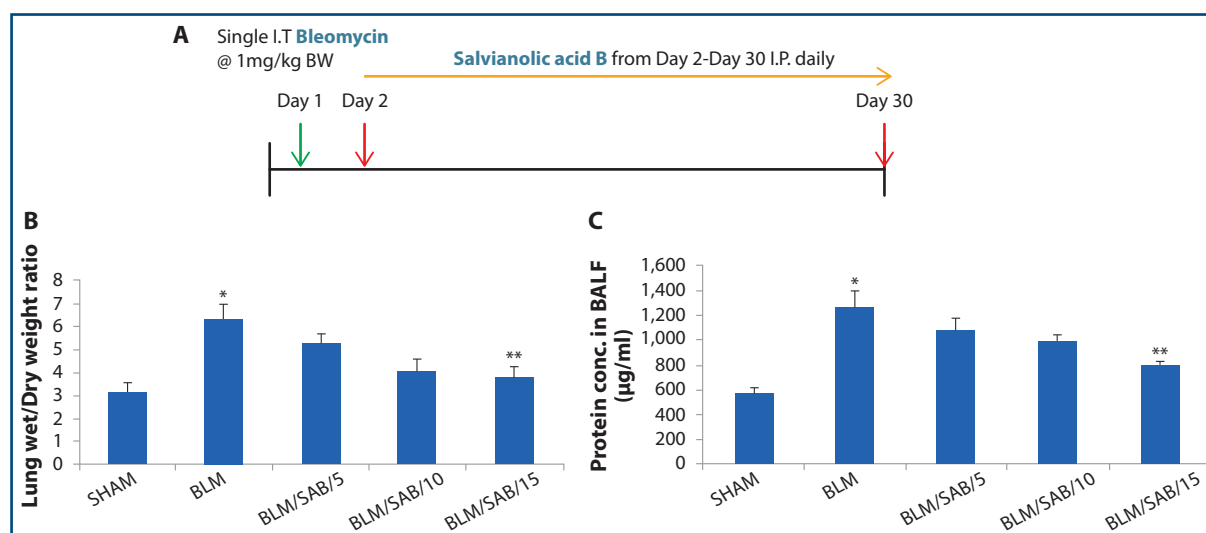


Figure 1. A. Schematic diagram representing the challenge and treatment given to the mice. **B, C.** Effect of Salvianolic acid B on bleomycin induced pulmonary edema and micro-vascular permeability. The wet dry (W/D) lung weight ratio was calculated as an indicator of pulmonary edema. Total protein concentration in bronchoalveolar lavage fluid (BALF) was estimated as a measure of vascular permeability. The data are mean \pm SE of six mice for each group. *P < 0.05 vs. SHAM group; **P < 0.05 vs. BLM group. Groups: SHAM/PBS (saline_only/control group), BLM (bleomycin @ 1 mg/kg group), BLM/SAB/5 (bleomycin/salvianolic acid B @ 5mg/kg), BLM/SAB/10 (bleomycin/ salvianolic acid B @ 10mg/kg) and BLM/SAB/15 (bleomycin/salvianolic acid B @ 15 mg/kg).

lung from each animal was taken and weighed immediately after its excision (wet weight). Then they were dried at 60 °C for 72 h, and weighed again. The wet dry (W/D) lung weight ratio was calculated as an indicator of pulmonary edema.

Estimation of protein in bronchoalveolar lavage fluid

Protein was estimated in BALF using commercially available BCA Protein Assay Kit (Thermo Scientific, USA) following the manufacturers protocol.

Histopathological studies

After BALF collection, lungs tissue samples were removed and fixed in 10% neutral buffered formalin. They were further routinely processed and embedded in paraffin. Five- μ m thick sections were stained with hematoxylin and eosin, Masson Trichrome and Picro-sirius red stainings for assessing the inflammation and fibrosis. The slides were viewed and photomicrographs were taken by microscope attached with camera (BX 61, Olympus Corporation and Japan). Lung injury assessment was performed by experimentally blind experts and graded semi-quantitatively using modified Ashcroft's scoring method (Hübner *et al.* 2008) with a score range of 0-8 score.

For Picro-sirius red staining, the slides were stained with picro-sirius red stain (0.1% Sirius red in aqueous saturated picric acid) for 1 hour followed by washing with acidified water (0.5% glacial acetic acid), dehydration and mounting with DPX. Collagen was red in colour while non-collagen components were orange. The images were analyzed using Image J (Fiji) software (<http://fiji.sc>). The intensity of the Masson Trichrome and picrosirius red positive area was expressed as percentage area (μm^2).

Estimation of lipid peroxidation and nitric oxide in lung homogenates

The lung (10 mg) were homogenised in 1 ml of ice-cold phosphate buffered saline (pH 7.4), using a tissue homogenizer with a teflon pestle at 4 °C. The resultant tissue homogenate was used for measurements of lipid peroxidation (LPO) and nitric oxide (NO) activity. LPO was determined in terms of malondialdehyde (MDA) production, by the thiobarbituric acid (TBA) method as described by Shafiqur-Rehman (Shafiqur-Rehman 1984). As an indicator of NO production, the nitrite concentration in lung homogenates of sacrificed animals was measured by using the Griess reagent. The amount of NO was expressed as nM/mg of protein formed per gram of wet tissue.

Estimation of myeloperoxidase (MPO) activity

Myeloperoxidase (MPO) activity was measured in lung homogenates using Myeloperoxidase Colorimetric Activity Assay Kit (SIGMA ALDRICH, St. Louis, USA) as per the manufacturer's instruction.

Estimation of cytokines by ELISA

Interleukin-6 (IL-6) and tumor necrosis factor- α (TNF- α) in BALF and transforming growth factor- β in lung homogenates were estimated using Mouse IL-6, Mouse TNF- α (KrishgenBiosystem), and Mouse Transforming Growth Factor- β (TGF- β) ELISA kits (YH Bioresearch Laboratory, China) as per the manufacturer instructions.

Estimation of transcription factor (NF- κ B) by ELISA

Nuclear factor kappa-light-chain-enhancer of activated B cells (NF- κ B) activity was measured in lung homogenates using Mouse NF- κ B ELISA kit (Shanghai Yehua Biological Technology co. Ltd. Shanghai, China) as per the manufacturer's instruction.

Assay of hydroxyproline

The collagen content in the lung homogenates was examined by a hydroxyproline assay. Briefly, 100 μ l of lung homogenate were hydrolyzed with equal amount of concentrated HCl in a pressure-tight, teflon capped vial at 120 °C for 3 hours followed clarification with activated charcoal. Ten μ l of each hydrolyzed sample were transferred to a 96-well plate and evaporate to dryness under vacuum. Hydroxyproline standard (1 mg/ml) was used to prepare the standard curve. Chloramine T reagent (100 μ l) was added to each sample and standard well. After 5 min incubation at room temperature, DMAB reagent (100 μ l) was added to each well and the plate was incubated for 90 min at 60 °C. The absorbance of each sample was read at 560 nm using a microplate reader.

Immunohistochemistry (IHC)

Immunohistochemical analysis for epithelial (E-cadherin) and mesenchymal markers (vimentin and α -smooth muscle actin) was performed (Singh *et al.* 2013). Briefly, 5- μ m paraffin sections on poly-L-lysine coated slides were rehydrated. After heat induced antigen retrieval and endogenous peroxidase blocking, the slides were incubated with primary antibodies to mouse monoclonal α -smooth muscle actin (Abcam, UK), Vimentin (Abcam, UK), and

to rabbit polyclonal E-cadherin (Gentex, USA). After incubation with secondary antibody (ABC, Universal, Vector), colour developed using diaminobenzidine (DAB) substrate and counterstained with haematoxylin. In negative control, tissue section was processed without application of primary antibody. Semi-quantitative immunohistochemical analysis was performed using scoring pattern as per Lomas and colleagues (Lomas *et al.* 2012) with a score range of 0-5 where 0 [0 Positives staining cells (%), no expression], 1 (< 1%, Negligible expression), 2 (1 to 10%, Scanty expression), 3 (10 to 33%, Low-moderate expression), 4 (33 to 66%, Moderate expression) and 5 (> 66%, Extensive expression).

Real-time PCR analyses of E-cadherin, α -smooth muscle actin and vimentin mRNA levels

For real-time PCR estimation of E-cadherin, α -smooth muscle actin and vimentin, lung tissues were preserved in RNA later (Qiagen) and immediately frozen at - 20 °C. RNA was extracted from these tissues using RNeasy mini kit (Qiagen, Germany) and cDNA was synthesised using Quantitect reverse transcription cDNA kit (Qiagen, Germany) as per the manufacturer's protocol. Real time PCR analyses of E-cadherin, α -smooth muscle actin and vimentin mRNA levels were done using primers specific for E-cadherin (forward: 5'-AAT GGC GGC AAT GCA ATC CCA AGA-3' and reverse: 5'-TGC CAC AGA CCG ATT GTG GAG ATA-3'); α -smooth muscle actin (forward: 5'-GGC TCT GGG CTC TGT AAG G-3' and reverse: 5'-CTC TTG CTC TGG GCT TCA TC-3') and vimentin (forward: 5'-GAG AAC TTT GCC GTT GAA GC-3' and reverse: 5'-GCTTCCTGT AGG TGG CAA TC-3'). GAPDH gene (forward 5'-CTG CAC CAC CAA CTG CTT AG-3' and reverse 5'-CCA GGA AAT GAG CTT GAC AAA-3') was taken as housekeeping gene for normalizing the expression data. Quantitative PCR was done in a 10 μ l reaction volume using a CFX C1000 real-time thermal cycler (Bio-Rad) with the SYBR green master mix (Qiagen) under the following amplification protocol: 95 °C for 6 min followed by 40 cycles of 95 °C for 20 seconds, 55 °C for 30 seconds and 72 for 20 seconds, followed by a melt curve analysis. A non template control (NTC) was run with every assay, and all determinations were performed at least in duplicates to achieve reproducibility. Results were analyzed with BioRAD Software and the relative quantitation was achieved by applying the comparative CT method. Average CT values were calculated from these replicates in each experimental condition. Relative quantification was carried out using the comparative CT ($\Delta\Delta$ CT) method. The relative fold change in the expression of a particular gene, as reflected in DNA level, between the different groups was calculated as Δ CT = CT target gene - CT endogenous control

and $\Delta\Delta$ CT = Δ CT test - Δ CT control. The amount of target, normalized to an endogenous reference and relative to a calibrator, is given by the formula: Fold change = $2^{-\Delta\Delta$ CT.

Ultrastructural examination of lung tissues

After animals were sacrificed, lung tissues were removed, dissected at size of 1 mm³ and fixed in Karnovsky's fixative for 6 hours at 4 °C. The tissues were processed for transmission electron microscopy as described earlier (Leishangthem *et al.* 2013). After several washing, the 1 mm³ lung tissues were post fixed in 1% osmium tetroxide for 1 hour at 4 °C followed by dehydrated at various grade of acetone (30-100% acetone) at 4 °C and clearing with 2 changes of toluene at room temperature and further processed and embedded in pure epoxy resin to make blocks. Ultrathin sections (70 nm) were mounted on the copper grid of 300 meshes size and stained with uranyl acetate and lead citrate. The sections were visualized with Tecnai 200 Kv transmission electron microscope (Tecnai, Fei Electron Optics) at All India Institute of Medical Science, New Delhi, India.

Statistical methods

Data generated from various experiments were presented as Mean \pm SE. All the grouped data were evaluated using SPSS/10.0 software. One-way analysis of variance (ANOVA) was used to detect differences among groups and the means were compared by Dunnett's post hoc test and a value of $P \leq 0.05$ was taken as significant.

Results

Pulmonary oedema and micro-vascular permeability

In the present study, the mean W/D lung weight ratio of BLM group (6.28 ± 0.65) showed significant ($p < 0.05$) increased in W/D mean lung weight ratio in comparison to the SHAM group (4.89 ± 0.46). BLM/SAB/15 group (3.74 ± 0.5) instead showed significant decreased in the W/D lung weight ratio as compared to that of BLM group. Moreover, mean W/D ratios of SHAM and BLM/SAB/15 did not differ significantly, indicating that SAB @ 15 mg/kg attenuated bleomycin induced lung oedema (Figure 1B).

Total protein concentration in BALF was estimated as a measure of vascular permeability. The mean total protein concentration in BALF of BLM ($1,251.25 \pm 137.60$ μ g/ml) was significantly

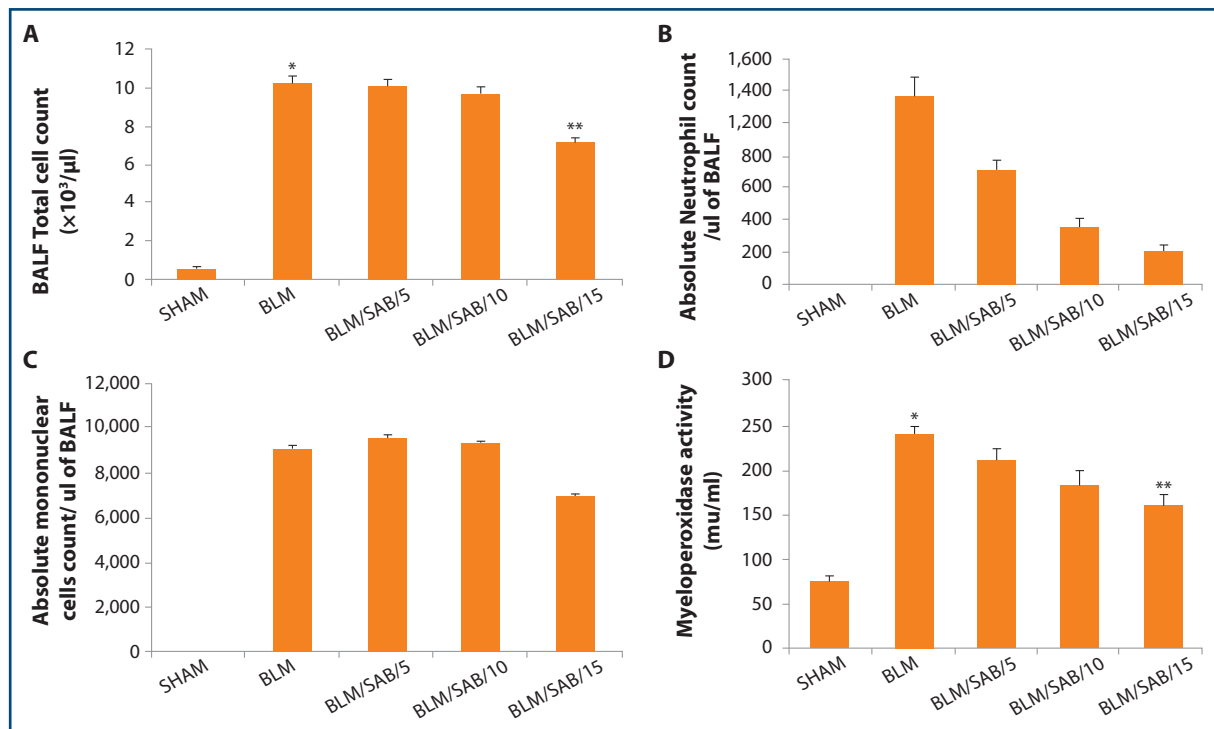


Figure 2. Effect of Salvianolic acid B on bleomycin induced pulmonary inflammatory cells infiltration. **A.** Total leukocytes count (TLC) in bronchoalveolar lavage fluid (BALF) of BLM group was increased significantly which were reduced in BLM/SAB/15. **B, C.** The cells were mainly of neutrophils followed by mononuclear cells. **D.** Myeloperoxidase (MPO) activity was measured as an indicator of polymorphonuclear leukocyte accumulation. The data are mean \pm SE of six mice for each group. * $P < 0.05$ vs. SHAM group; ** $P < 0.05$ vs. BLM group. Groups: SHAM/PBS (saline_only/control group), BLM (bleomycin @ 1 mg/kg group), BLM/SAB/5 (bleomycin/salvianolic acid B @ 5mg/kg), BLM/SAB/10 (bleomycin/ salvianolic acid B @ 10mg/kg) and BLM/SAB/15 (bleomycin/salvianolic acid B @ 15 mg/kg).

($p < 0.05$) higher as compared to that of SHAM ($573.42 \pm 44.6 \mu\text{g/ml}$). However, BLM/SAB/15 ($806.3 \pm 22.02 \mu\text{g/ml}$) showed significant reduction in total protein concentration as compared to that of BLM group (Figure 1C).

Pulmonary inflammatory cell infiltration

In the present study inflammatory cell infiltration in bleomycin induced lung injury was assessed by analysis of total leukocyte count (TLC) and differential leukocyte count (DLC) in BALF and by estimation of MPO activity in lung homogenates (Figure 2). There was a massive surge in the mean TLC in BALF of BLM ($10.25 \pm 0.32 \times 10^3/\mu\text{l}$) group as compared to SHAM ($0.57 \pm 0.08 \times 10^3/\mu\text{l}$). In contrast, TLC of BLM/SAB/15 group ($7.15 \pm 0.24 \times 10^3/\mu\text{l}$) showed marked reduction in the total numbers of inflammatory cells (Figure 2A). There was no significant difference in BLM/SAB/5 ($10.1 \pm 0.27 \times 10^3/\mu\text{l}$) and BLM/SAB/10 ($9.67 \pm 0.37 \times 10^3/\mu\text{l}$) groups. Furthermore, there was decrease in the absolute count of neutrophils mononuclear cell in SAB treated group @ 15 mg/kg as compared to BLM group.

The mean values of MPO activity in lung homogenates were significantly higher in BLM group ($242.19 \pm 8.49 \text{ mU/ml}$) as compared to SHAM

($75.15 \pm 5.54 \text{ mU/ml}$). However, BLM/SAB/15 group ($160.58 \pm 12.64 \text{ mU/ml}$) showed significant reduction in the MPO activity as compared to BLM group.

Level of NF-kB activity

In BLM group, the NF-kB activity level in lung homogenates was increased to $7.74 \pm 0.4 \text{ ng/ml}$ as compared to SHAM group ($4.3 \pm 0.52 \text{ ng/ml}$). But this decreased significantly in BLM/SAB/15 ($5.52 \pm 0.16 \text{ ng/ml}$) (Figure 3).

Inflammatory cytokine production

The proinflammatory cytokines TNF- α and IL-6 were estimated in BALF (Figure 4). There was a massive increase in the level of TNF- α in BLM when compared to SHAM group. Conversely, the level was significantly lower in BLM/SAB/15 group as compared to BLM group. Further, there was also significant increase in the level of IL-6 in BLM group compared to SHAM. Dose dependent reduction in IL-6 level was also seen in BLM/SAB/15 group.

Oxidative stress

The malondialdehyde levels (nM MDA/g) were

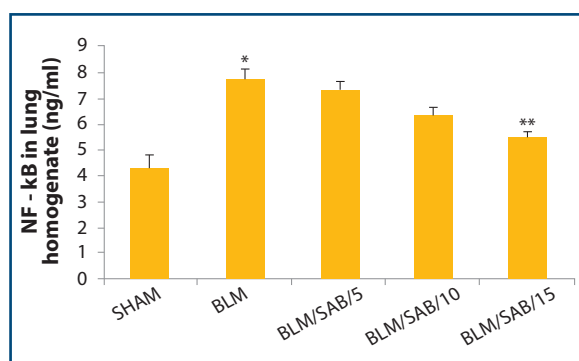


Figure 3. Effect of Salvianolic acid B on bleomycin induced nuclear factor kappa-light-chain-enhancer of activated B cells (NF-kB) level in bronchoalveolar lavage fluid (BALF) of different groups of mice. Salvianolic acid B attenuated bleomycin induced transcription activity. The data are mean \pm SE of six mice for each group. *P < 0.05 vs. SHAM group; **P < 0.05 vs. BLM group. Groups: SHAM/PBS (saline_only/control group), BLM (bleomycin @ 1 mg/kg group), BLM/SAB/5 (bleomycin/salvianolic acid B @ 5mg/kg), BLM/SAB/10 (bleomycin/salvianolic acid B @ 10mg/kg) and BLM/SAB/15 (bleomycin/salvianolic acid B @ 15 mg/kg).

estimated as an indicator of lipid peroxidation. The lung MDA level of BLM group was raised to 3.19 ± 0.50 nM MDA/g in comparison to control group. BLM/SAB/15 group showed decreased in MDA level (1.96 ± 0.08 nM MDA/g) as compared to that of BLM group (Figure 5A). Further, nitric oxide activity was significantly increased in BLM group (15.38 ± 0.3 nM/mg of protein) as compared to SHAM (7.48 ± 0.24 nM/mg). However, there was significant decrease in NO activity in BLM/SAB/15 group (10.42 ± 0.47 nM/mg) as compared to that of BLM group (Figure 5B).

Histopathological changes

Histopathological examination of the lung section showed infiltration of the inflammatory cells (mononuclear cells and neutrophils) in alveolar, perivascular and peribronchiolar areas along with fibrosis and collagen deposition indicating chronic

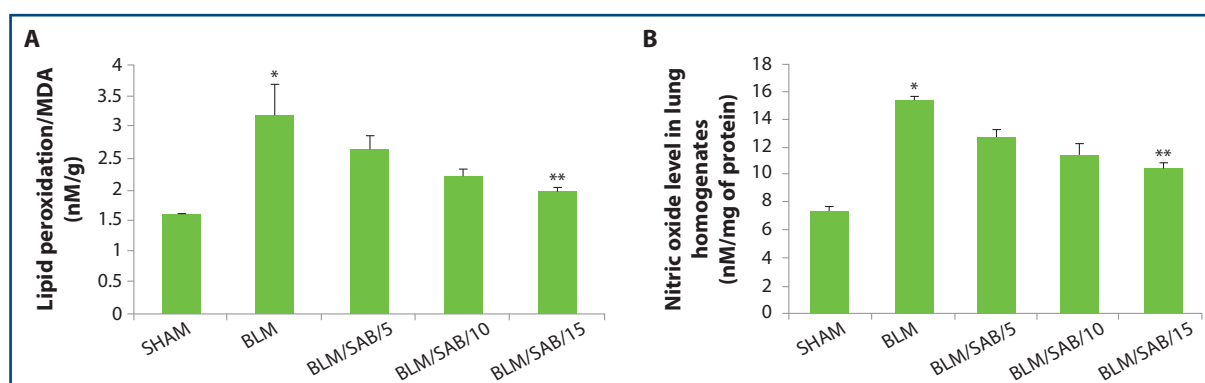


Figure 4. Effect of Salvianolic acid B on bleomycin induced oxidative/nitrosative stress. Salvianolic acid B attenuated bleomycin induced oxidative stress by lowering the lipid peroxidation and nitric oxide level which was increased in BLM groups. The data are mean \pm SE of six mice for each group. *P < 0.05 vs. SHAM group; **P < 0.05 vs. BLM group. Groups: SHAM/PBS (saline_only/control group), BLM (bleomycin @ 1 mg/kg group), BLM/SAB/5 (bleomycin/salvianolic acid B @ 5mg/kg), BLM/SAB/10 (bleomycin/salvianolic acid B @ 10mg/kg) and BLM/SAB/15 (bleomycin/salvianolic acid B @ 15 mg/kg).

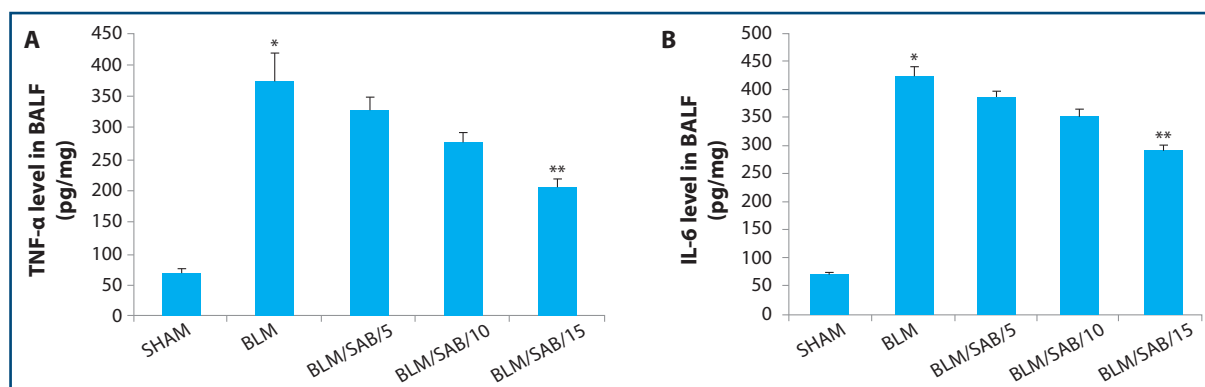


Figure 5. Effect of Salvianolic acid B on bleomycin induced proinflammatory cytokines production. Salvianolic acid B attenuated bleomycin induced inflammatory cytokine (TNF- α and IL-6) production. The data are mean \pm SE of six mice for each group. *P < 0.05 vs. SHAM group; **P < 0.05 vs. BLM group. Groups: SHAM/PBS (saline_only/control group), BLM (bleomycin @ 1 mg/kg group), BLM/SAB/5 (bleomycin/salvianolic acid B @ 5mg/kg), BLM/SAB/10 (bleomycin/salvianolic acid B @ 10mg/kg) and BLM/SAB/15 (bleomycin/salvianolic acid B @ 15 mg/kg).

inflammation in BLM mice as compared to SHAM mice which showed normal architecture of lungs with bronchioles and alveoli (Figure 6A-6B). The pathological changes significantly improved in BLM/SAB/15 group when compared to BLM (Figure 6C). Assessment of pulmonary morphological changes by Ashcroft's scoring scale showed reduced score in SAB treated groups as compared to BLM group (Figure 6D).

Pulmonary fibrosis

In the present study, the TGF- β levels in BLM group significantly increased (600.28 ± 62.98 pg/mg) as compared to SHAM (111.87 ± 7.43 pg/mg). SAB treated groups showed significant reduction in TGF- β 1 levels. The maximum reduction was observed in BLM/SAB/15 group (335.34 ± 31.55 pg/mg) as compared to BLM group (Figure 7A). Further, lung collagen levels were determined by hydroxyproline assay in lung homogenates. BLM group showed significantly higher level of hydroxyproline as compared to SHAM (0.3 ± 0.01 μ g/mg). The level significantly decreased in BLM/SAB/15 groups. Hence, this signifies that SAB could

attenuate collagen deposition in lungs (Figure 7B). Moreover, by Masson's trichrome (Figure 8A-8D) and Picro-sirius red (Figure 9A-9D) staining, there was decreased fibrosis in SAB treated groups. Score of Masson's trichrome and picrosirius red stained section in % area was higher in BLM as compared to that of SHAM group. But was reduced in BLM/SAB/15 group (Figure 8D and 9D). The decrease was more pronounced in BLM/SAB/15 group suggesting the anti-fibrotic role of SAB in dose dependent manner.

Changes in the expression of EMT markers

In the present study, immunohistochemical studies were done using primary antibodies against epithelial (E-cadherin) and mesenchymal (vimentin and α -smooth muscle actin) markers. In BLM group, the expression of E-cadherin was reduced. SHAM group showed expression of E-cadherin in the cytoplasm of the bronchial and alveolar epithelial cells with overall score of 4.41 ± 0.07 , BLM group instead expressed E-cadherin (2.27 ± 0.08) mainly on the tip of bronchial epithelial cells (Figure 10A-10B). SAB treatment was able to restore the expression of

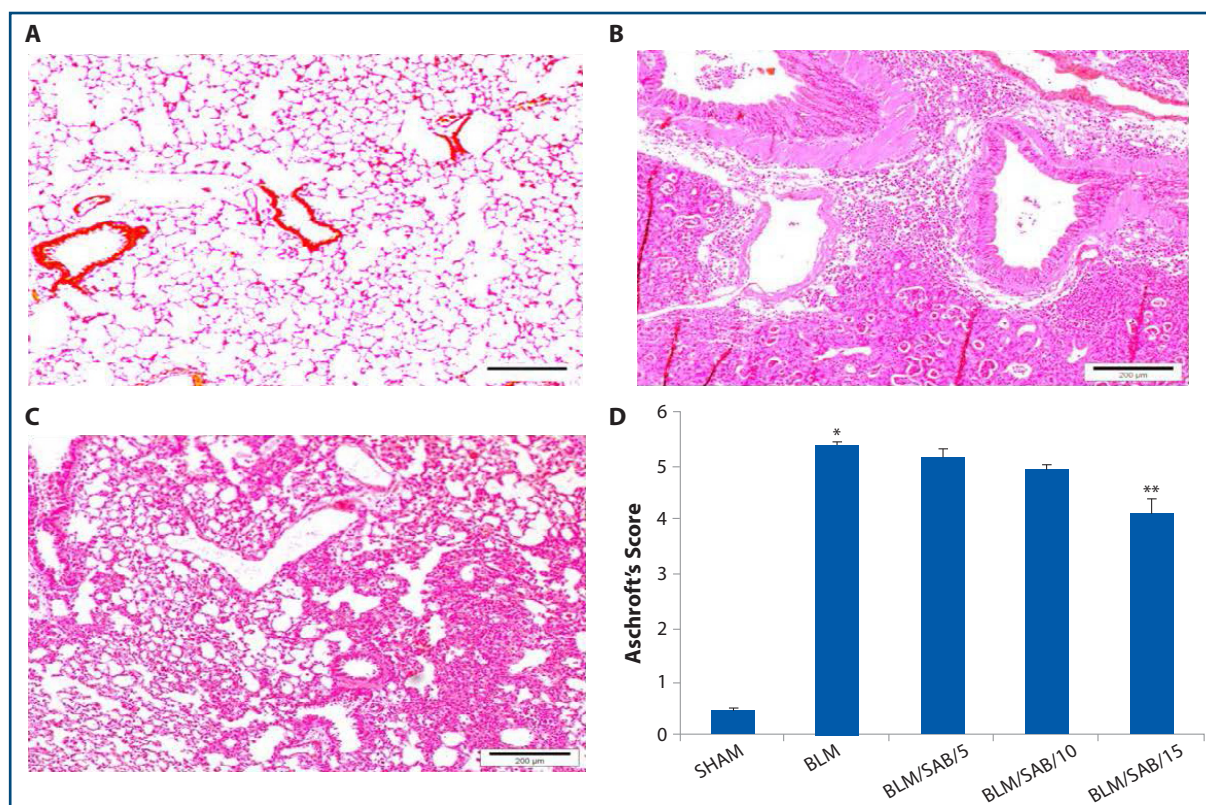


Figure 6. Representative photomicrograph showing histopathological features of lungs in different groups. **A.** SHAM group showed normal lung architecture. **B.** There was infiltration of inflammatory cells within the alveolar areas. **C.** Histopathological features of lungs in BLM/SAB/15 showed significant alleviation of BLM induced lung inflammation and fibrosis. (H&E, bar = 200 μ m) **D.** Ashcroft's scoring for assessment of histological changes of different groups of mice. Lung injury was higher in BLM group which was decreased in SAB treated groups. The data are mean \pm SE of six mice for each group. *P < 0.05 vs. SHAM group; **P < 0.05 vs. BLM group. Groups: SHAM/PBS (saline_only/control group), BLM (bleomycin @ 1 mg/kg group), BLM/SAB/5 (bleomycin/salvianolic acid B @ 5mg/kg), BLM/SAB/10 (bleomycin/ salvianolic acid B @ 10mg/kg) and BLM/SAB/15 (bleomycin/salvianolic acid B @ 15 mg/kg).

E-cadherin (3.33 ± 0.04) in bronchial and alveolar epithelial cells (Figure 10C).

α -SMA is normally expressed in the bronchial as well

as vascular smooth muscles as observed in SHAM mice (1.36 ± 0.05). Conversely, in the BLM group (3.8 ± 0.1), there was an increased immunolocalization

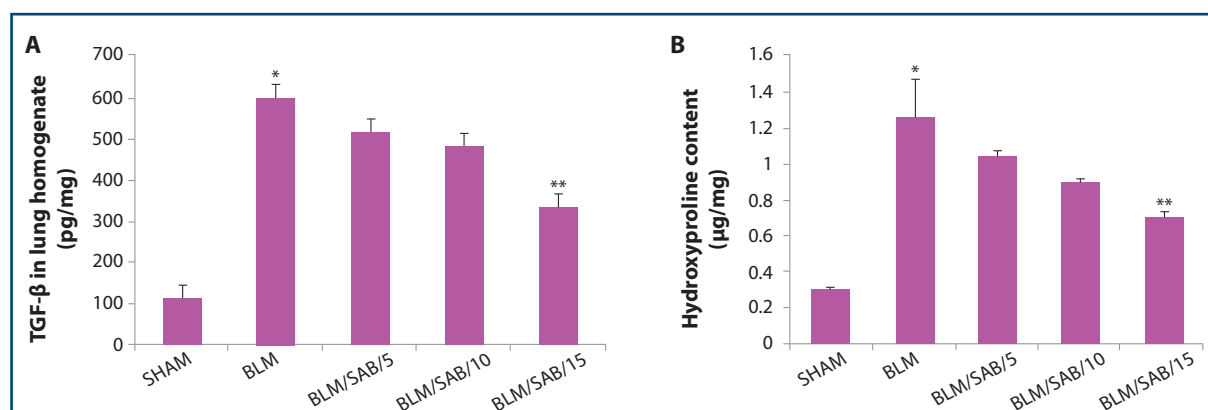


Figure 7. Effect of Salvianolic acid B on bleomycin induced Transforming Growth Factor- β (TGF β) levels and hydroxyproline content in lung homogenates of different groups of mice. Salvianolic acid B attenuated bleomycin induced TGF- β production. The collagen content in the lung homogenates was examined by a hydroxyproline assay. The data are mean \pm SE of six mice for each group. *P < 0.05 vs. SHAM group; **P < 0.05 vs. BLM group. Groups: SHAM/PBS (saline_only/control group), BLM (bleomycin @ 1 mg/kg group), BLM/SAB/5 (bleomycin/salvianolic acid B @ 5mg/kg), BLM/SAB/10 (bleomycin/ salvianolic acid B @ 10mg/kg) and BLM/SAB/15 (bleomycin/salvianolic acid B @ 15 mg/kg).

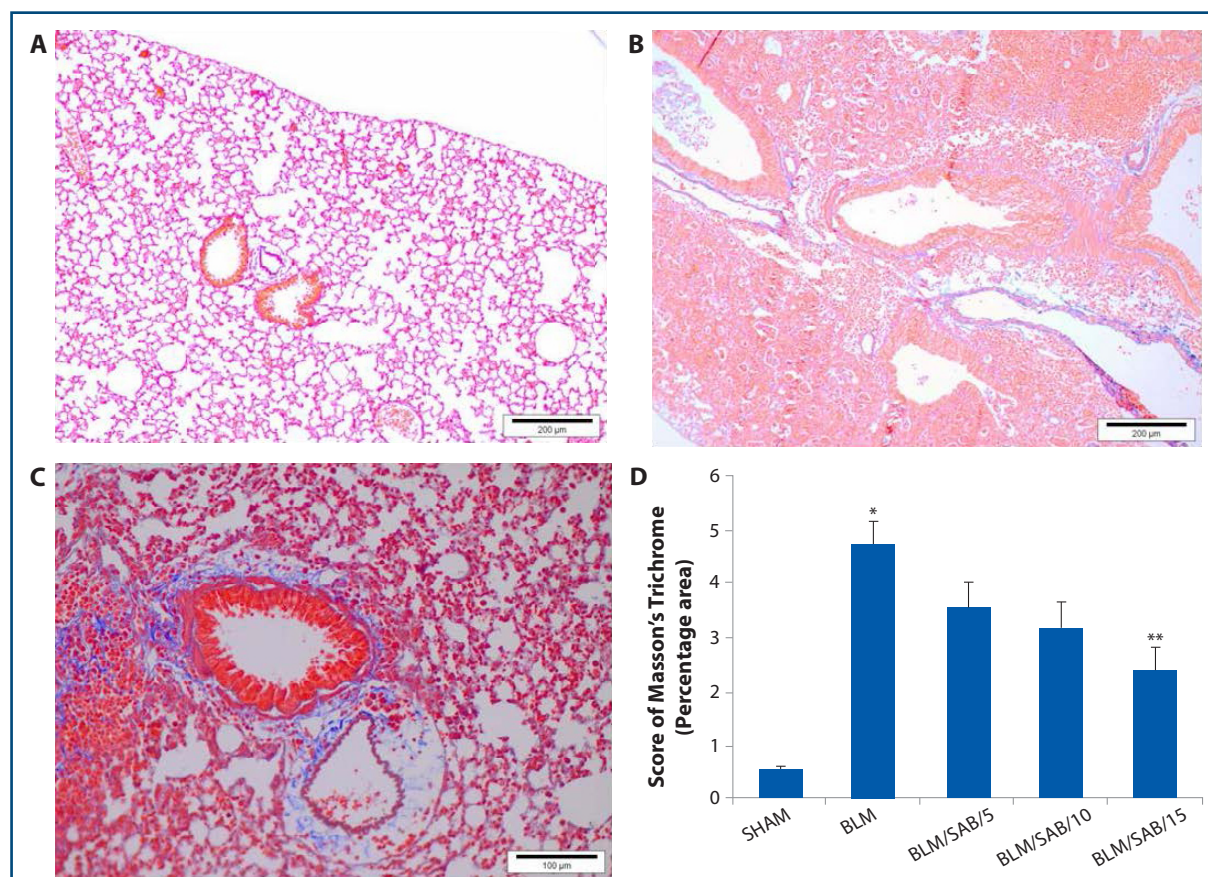


Figure 8. Representative photomicrograph of Masson's Trichrome stained lung section. **A.** SHAM mice showed normal histology with normal alveolar architecture (bar = 200 μ m). **B.** BLM mice showing collagen deposition (blue colour) in interstitial area (bar = 200 μ m). **C.** BLM/SAB/15 showed decreased collagen deposition as compared to BLM with improved lung architecture (Masson's trichrome stain, bar = 100 μ m). **D.** Masson's Trichrome score was higher in BLM group which was decreased in SAB treated groups. The data are mean \pm SE of six mice for each group. *P < 0.05 vs. SHAM group; **P < 0.05 vs. BLM group. Groups: SHAM/PBS (saline_only/control group), BLM (bleomycin @ 1 mg/kg group), BLM/SAB/5 (bleomycin/ salvianolic acid B @ 5mg/kg), BLM/SAB/10 (bleomycin/ salvianolic acid B @ 10mg/kg) and BLM/SAB/15 (bleomycin/salvianolic acid B @ 15 mg/kg).

of α -SMA in the myofibroblasts within the alveolar interstitial area which was further restored by SAB treatment (2.33 ± 0.06) (Figure 11A-11C). Similarly, BLM group (3.83 ± 0.09) showed increased

expression of vimentin within the alveolar interstitial areas as well as alveolar macrophages in contrast to SHAM group (0.05 ± 0.03) which showed low or negligible expression of vimentin. SAB treatment

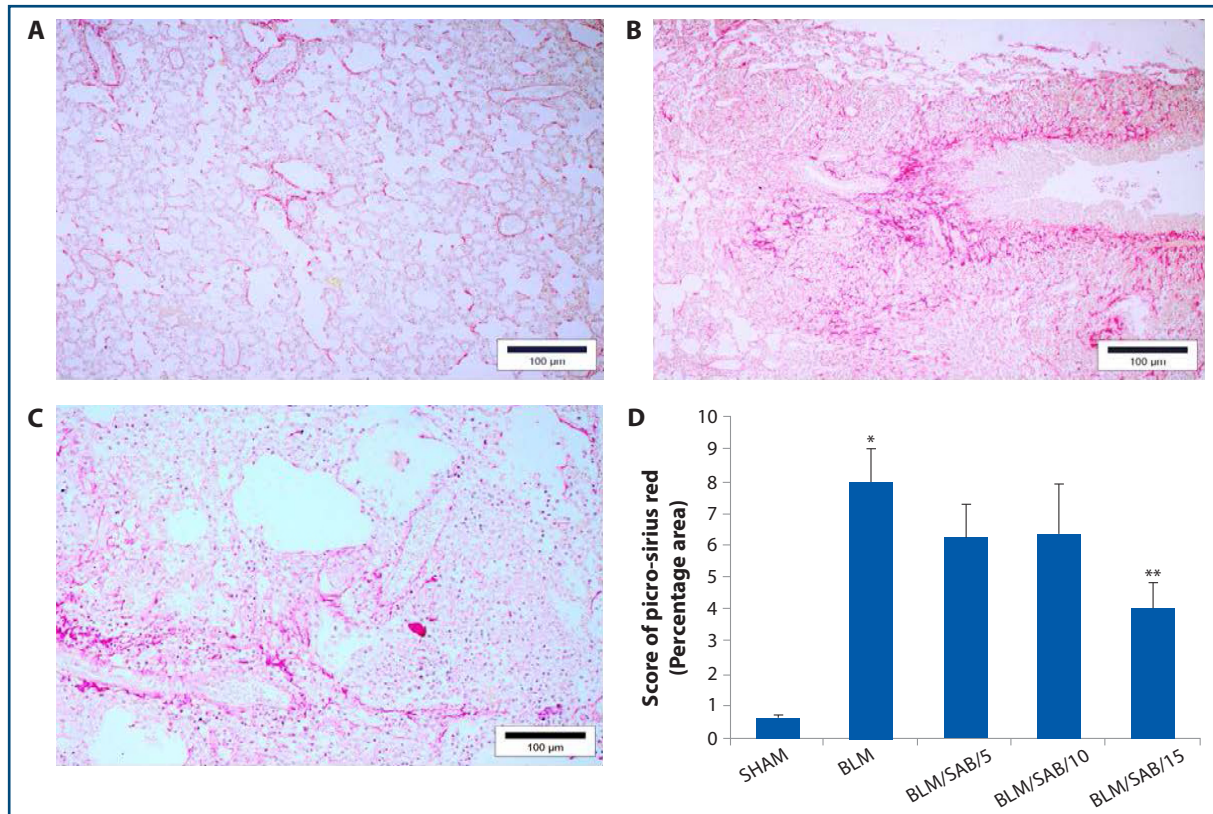


Figure 9. Representative photomicrograph of Picro-Sirius red stained lung section. **A.** SHAM mice showed normal architecture of lung with normal alveoli and normal bronchioles. **B.** BLM mice showing heavy collagen deposition in interstitial area. **C.** BLM/SAB/15 mice showed normal alveoli with mild deposition in interstitial spaces (Picro-Sirius red, bar = 100 μ m). **D.** Picro-Sirius red score was higher in BLM group which was decreased in SAB treated groups. The data are mean \pm SE of six mice for each group. *P < 0.05 vs. SHAM group; **P < 0.05 vs. BLM group. Groups: SHAM/PBS (saline_only/control group), BLM (bleomycin @ 1 mg/kg group), BLM/SAB/5 (bleomycin/salvianolic acid B @ 5mg/kg), BLM/SAB/10 (bleomycin/salvianolic acid B @ 10mg/kg) and BLM/SAB/15 (bleomycin/salvianolic acid B @ 15 mg/kg).

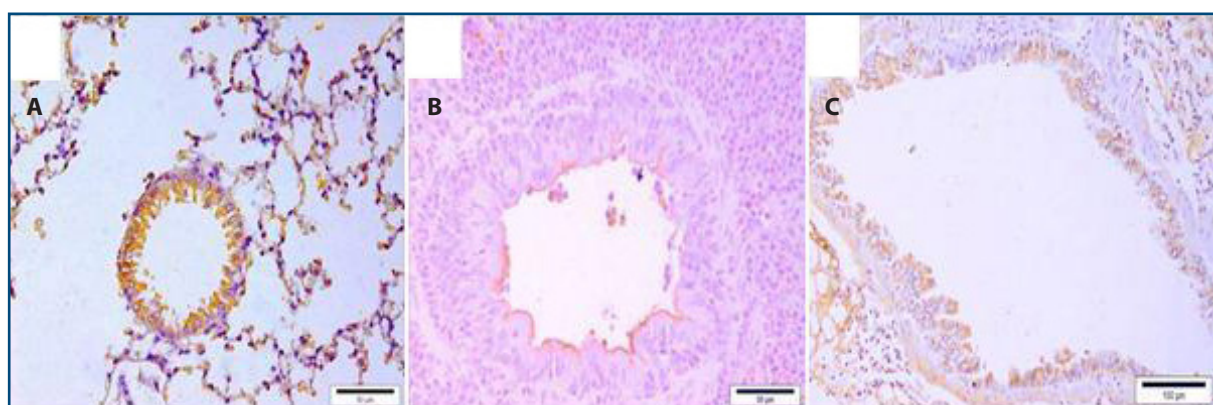


Figure 10. Representative photomicrograph of lung showing immunolocalization of E-cadherin. **A.** Representative photomicrograph of lung showing highly expressed E-cadherin in the cytoplasm of the bronchial epithelial cells and alveolar epithelial cells in SHAM group (brown colour). **B.** BLM group showing reduced expression of E-cadherin and were expressed on the tip of the bronchial epithelial cells. **C.** BLM/SAB/15 group restored the expression of E-cadherin in the epithelial cells (Immunohistochemistry, bar = 50 μ m). Groups: SHAM/PBS (saline_only/control group), BLM (bleomycin @ 1 mg/kg group), BLM/SAB/5 (bleomycin/salvianolic acid B @ 5mg/kg), BLM/SAB/10 (bleomycin/salvianolic acid B @ 10mg/kg) and BLM/SAB/15 (bleomycin/salvianolic acid B @ 15 mg/kg).

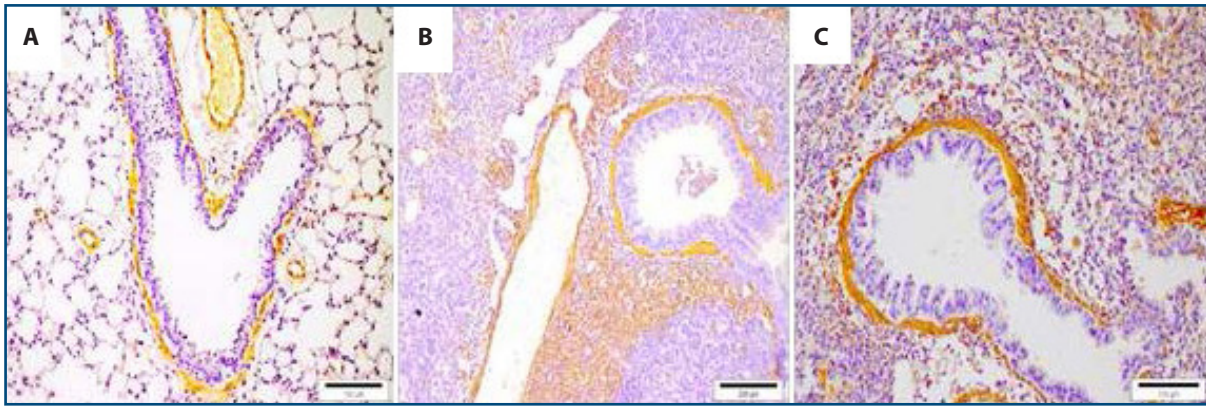


Figure 11. Representative photomicrograph of lung showing immunolocalization of alpha- smooth muscle actin. **A.** SHAM groups showed alpha-smooth muscle actin normally expressed in the bronchial as well as vascular smooth muscles. **B.** BLM groups showed increased expression of alpha- smooth muscle actin in the alveolar interstitial areas. **C.** BLM/SAB/15 groups showed reduced expression of alpha- smooth muscle actin in the alveolar interstitial areas (Immunohistochemistry, bar=100 μ m). Groups: SHAM/PBS (saline_only/control group), BLM (bleomycin @ 1 mg/kg group), BLM/SAB/5 (bleomycin/salvianolic acid B @ 5mg/kg), BLM/SAB/10 (bleomycin/ salvianolic acid B @ 10mg/kg) and BLM/SAB/15 (bleomycin/ salvianolic acid B @ 15 mg/kg).

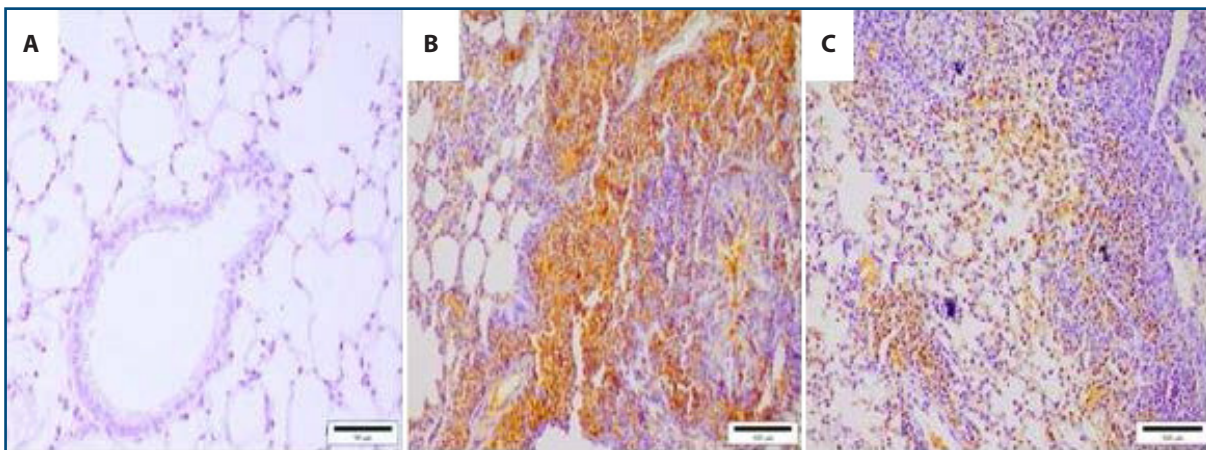


Figure 12. Representative photomicrograph of lung showing immunolocalization of vimentin. **A.** SHAM mice showed very low to negligible expression of vimentin. **B.** BLM group showed higher expression of vimentin in the alveolar interstitial areas as well as in perivascular and peribronchiolar areas. **C.** Representative photomicrograph of lung in BLM/SAB/15 group showed reduction in the expression of vimentin. (Immunohistochemistry, bar=100 μ m). Groups: SHAM/PBS (saline_only/control group), BLM (bleomycin @ 1 mg/kg group), BLM/SAB/5 (bleomycin/salvianolic acid B @ 5mg/kg), BLM/SAB/10 (bleomycin/ salvianolic acid B @ 10mg/kg) and BLM/SAB/15 (bleomycin/salvianolic acid B @ 15 mg/kg).

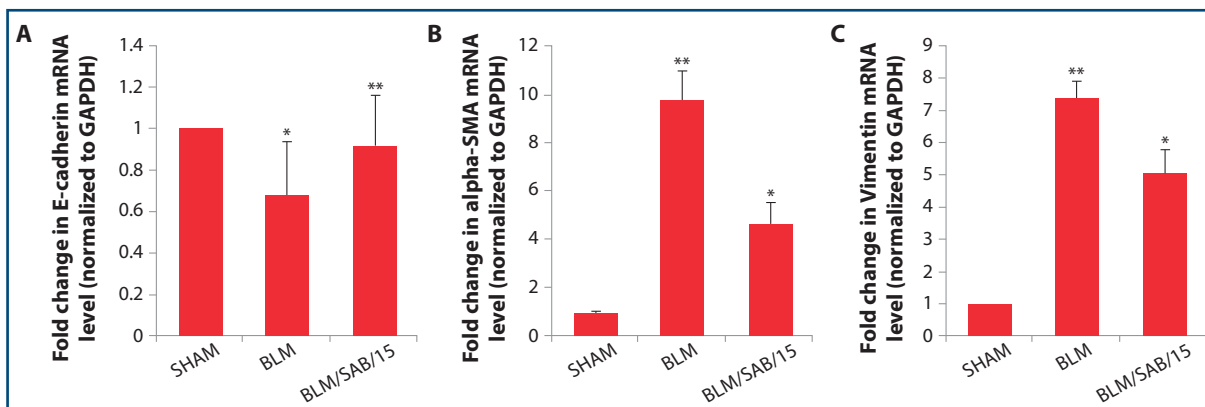


Figure 13. Real-time PCR analysis of E-cadherin, alpha- smooth muscle actin (SMA) and vimentin mRNA level in lungs. The data are mean \pm SE of six mice for each group. *P < 0.05 vs. SHAM group; **P < 0.05 vs. BLM group. Groups: SHAM/PBS (saline_only/control group), BLM (bleomycin @ 1 mg/kg group), BLM/SAB/5 (bleomycin/salvianolic acid B @ 5mg/kg), BLM/SAB/10 (bleomycin/ salvianolic acid B @ 10mg/kg) and BLM/SAB/15 (bleomycin/salvianolic acid B @ 15 mg/kg).

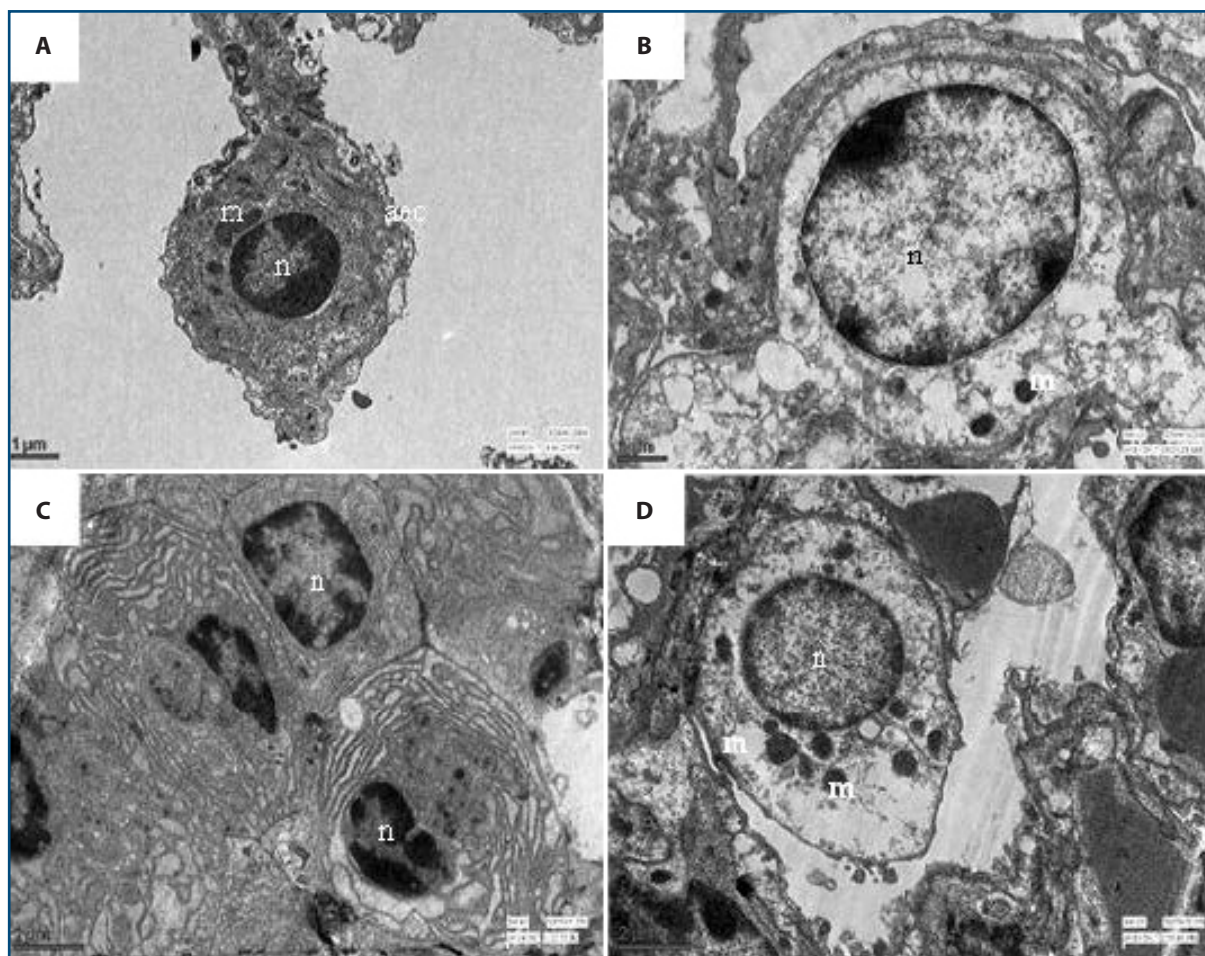


Figure 14. Representative ultrastructural photomicrograph of the lungs. **A.** Alveolar epithelial cells with normal nucleus in SHAM. **B.** Apoptotic type 2 pneumocyte/alveolar epithelial cells with loss of mitochondria and vacuolation in BLM group. **C.** BLM group showing infiltrating inflammatory cells which were mainly plasma cells with rough endoplasmic reticulum. **D.** BLM/SAB/15 group showed restoration of injury to alveolar epithelial cells with improvement in the mitochondrial damage (n=nucleus, aec=alveolar epithelial cell, m-mitochondria). Groups: SHAM/PBS (saline_ only/control group), BLM (bleomycin @ 1 mg/kg group), BLM/SAB/5 (bleomycin/salvianolic acid B @ 5mg/kg), BLM/SAB/10 (bleomycin/ salvianolic acid B @ 10mg/kg) and BLM/SAB/15 (bleomycin/salvianolic acid B @ 15 mg/kg).

reduced the expression of vimentin (2.30 ± 0.05) (Figure 12A-12C).

In addition, in BLM group the expression of E-cadherin mRNA levels in lungs was reduced by 0.6 ± 0.25 fold. The level of α -SMA increase up to 9.71 ± 1.20 fold while that of vimentin increased 7.39 ± 0.52 fold in as compared to that of SHAM. In BLM/SAB/15 group, the mRNA level of E-cadherin was restored up to 0.92 ± 0.24 fold that of the α -SMA to 4.64 ± 0.85 and that of vimentin to 5.03 ± 0.73 (Figure 13A-13C).

Ultrastructural changes

Ultrastructural changes in alveolar epithelial cells were studied by using transmission electron microscopy (Figure 14 A-D). Severe degeneration of alveolar epithelial cells was observed with loss of mitochondria as vacuolations. There was also a presence of collagen fibres deposition around the

alveolar epithelial cells. The infiltrating mononuclear cells were mainly plasma cells. These changes were alleviated in BLM/SAB/15 group where alveolar epithelial cells showed restoration of mitochondrial damage.

Discussion

Pulmonary fibrosis is the end stage of many diffuse parenchymal lung diseases characterized by excessive accumulation of ECM within the pulmonary interstitium leading to progressive and irreversible destruction of the normal lung architecture and finally respiratory insufficiency (Todd *et al.* 2012). Pulmonary fibrosis is characterized by slowly progressive fibrotic foci that involve inappropriately activated (myo) fibroblasts that are responsible for development of fibrosis (Rosenbloom *et al.* 2017).

Salvianolic acid B has been widely accepted in the

treatment of various diseases on account of its anti-inflammatory, anti-oxidative, anti-proliferative, and anti-fibrotic properties (Chen *et al.* 2016, Liu *et al.* 2016). There were few studies on the therapeutic use of SAB against BLM induced pulmonary fibrosis (Liu *et al.* 2015, Liu *et al.* 2016) where they targeted mainly on the TGF- β pathways related mechanism. Here in the present study, all the areas from inflammation, oxidative stress, NF- κ B activity, EMT markers along with light and ultra-structural changes associated with bleomycin induced lung injury and its amelioration with Salvianolic acid B were covered.

Bleomycin caused endothelial cell injury and increased microvascular permeability resulting in the sudden onset of pulmonary oedema of non-cardiogenic origin characterized by a considerable and rapid accumulation of protein rich oedematous fluid into the alveolar space (Ware and Matthay 2000). Increase in the endothelial barrier permeability by bleomycin could be due to TNF- α secreted by macrophages recruited at the site of injury that might have induced tyrosine phosphorylation of cell junction proteins leading to interstitial oedema and inflammation in lung microvasculature (Dejana *et al.* 2008). In the present study, bleomycin induced pulmonary oedema and microvascular permeability was attenuated by SAB representing its anti-inflammatory property. SAB has alleviative effect on pulmonary edema in rats with sepsis (Yang *et al.* 2018).

In interstitial lung disease, alveolar and interstitial inflammation by inflammatory cell infiltration is essential for the development of lung injury and subsequent fibrosis. In BLM groups, the TLC was increased and these cells were mainly mononuclear cells along with neutrophils. This may be due to infiltration of the neutrophils followed by sustained increase in mononuclear cells like macrophages and lymphocytes during BLM induced lung injury (Izbicki *et al.* 2002). Further, there was significant increase in MPO activity in BLM group as compared to control group. This might be attributed to the fact that in the sub-acute stage, macrophages and to a lesser extent neutrophils form a part of inflammatory exudate and both secrete MPO. Maretta and colleagues (Maretta *et al.* 2014) showed that alveolar macrophages expressed MPO in acute respiratory distress syndrome. In addition, in the development of BLM-induced pulmonary fibrosis, TNF- α expression triggers both initial acute inflammatory response to tissue damage as well as chronic inflammatory signals required for collagen deposition (Oikonomou *et al.* 2006). IL-6 instead functions as a proinflammatory factor as well as a profibrotic factor (Saito *et al.* 2008). These findings suggest that the protective effect of SAB in pulmonary injury may be, at least in part, attributed to the suppression of inflammatory cell

sequestration and infiltration into lungs, in turn attenuating pro-inflammatory cytokine release.

Bleomycin binds to iron (Fe^{2+}), undergoes redox cycling and catalyzes the formation of ROS that plays a major role in the progression of pulmonary fibrosis by targeting DNA, protein and lipids with ultimate progression of lipid peroxidation (Martin and Kachel 1987). SAB being an antioxidant reduced the LPO production which may be due to scavenging of free radicals 1, 1-diphenyl-2-picrylhydrazyl (DPPH) in the blood stream leading to reduced direct injury to pulmonary vascular endothelium (Wu *et al.* 1998). Nitric oxide plays an important role in maintaining respiratory homeostasis (Sugiura and Ichinose 2011, Ricciardolo *et al.* 2004). Nitric oxide is also involved in the pathophysiology of several pulmonary diseases when there is any subtle variations in its rate of production from alveolar macrophages leading to inflammatory response and tissue damage (Philippe *et al.* 1991). Salvianolic acid B showed neuroprotective effect in microglia by reduction of NO production Wang and colleagues (Wang *et al.* 2010).

Nuclear factor- κ B plays a significant role in the development of bleomycin induced lung toxicity. Bleomycin induced the transcriptional activation of NF- κ B signalling in human bronchial epithelial cells (Ma *et al.* 2009). Further, exposure of cells to bleomycin trigger the activation of NF- κ B by the release of proinflammatory cytokines like TNF- α , and IL-1 β . In the present study, SAB treatment reduced bleomycin induced NF- κ B activity. This may be due to suppression of BLM-induced TNF- α , and IL-1 β mRNA expression, accompanied by decrease in phosphorylated I κ B- α (Inhibitory κ B α) level and NF- κ B p65 protein level leading to inhibition of transcription factor NF- κ B activation (Wang *et al.* 2010, Xia *et al.* 2018). Thus, in our study, the decreased activity of oxidative/nitrosative stress as well as NF- κ B activation by SAB again specifies its anti-inflammatory property.

Histopathological examinations demonstrated infiltration of mononuclear cells and neutrophils in interstitial area as well as in alveolar area, and deposition of excessive fibrin in interstitial tissue of BLM groups which was restored by SAB treatment that could obviously lower the degree of alveolitis and lung fibrosis. Furthermore, antifibrotic effect of SAB in BLM-induced pulmonary fibrosis was observed as shown by reduced deposition of collagen as presented by Masson's trichrome, Picro-sirius red stained lung sections as well as hydroxyproline content in the lung. Moreover, in the present study the level of TGF- β was increased in BLM groups which were lowered with SAB treatment. TGF- β is produced by inflammatory and epithelial cells and plays a central role in idiopathic

pulmonary fibrosis and airway remodelling (Tatler and Jenkins 2012). Liu and colleagues (Liu *et al.* 2016) showed that SAB attenuates experimental pulmonary fibrosis through inhibition of the TGF- β signaling pathway.

During EMT, epithelial cells lose their distinct marker expression profile like E-cadherin and acquire a mesenchymal morphology associated with expression of fibroblastic markers particularly α -SMA, type I and III collagen, vimentin (Jinde *et al.* 2001, Rastaldi *et al.* 2002, Nishitani *et al.* 2005). E-cadherin, a cell adhesion molecule, normally expressed by epithelial cells is repressed during EMT. In the present study, the expression of E-cadherin was suppressed in BLM group. This may be due to the fact that TGF- β represses E-cadherin production in epithelial cells (Choi *et al.* 2007).

Moreover, α -SMA plays an important role in fibrogenesis (Kawasaki *et al.* 2008) and α -SMA positive myofibroblasts have been demonstrated in type 2 EMT associated with tissue regeneration and organ fibrosis (Zeisberg *et al.* 2003). Stressed and injured epithelium can give rise to myofibroblasts and thereby contribute to fibrogenesis (Lee and Nelson 2012). Myofibroblasts phenotype characterized by increased expression of the α -SMA protein is the major producers of the ECM. In a self-limiting pulmonary fibrosis, myofibroblasts gradually disappear as the active fibrotic phase is terminated. In contrast, these cells persist and can be found in various fibrotic conditions, including pulmonary fibrosis where the disease is progressive (Kuhn and McDonald 1991). Thus in the present study there was increase expression of mesenchymal markers, α -SMA and vimentin in the interstitial areas which was restored by SAB treatment. Moreover, in the present study TGF- β level was higher in BLM groups which were reduced by SAB treatment. This might be due to blocking of TGF- β -mediated upregulation of α -SMA and vimentin by SAB (Yang *et al.* 2015). TGF- β is also a potent activator of myofibroblasts which expressed α -SMA (Desmoulière 1995). Vimentin coordinates fibroblast proliferation and keratinocyte differentiation in wound healing via TGF- β -Slug signalling (Cheng *et al.* 2016). Grande and his co-workers (Grande *et al.* 2015) stated that Snail1 caused partial EMT of type 2 in renal fibrosis, where there is confinement of the damaged adult epithelial cells to their tissue of origin, without involvement in the delamination and invasion programs. Lovisa and his colleagues (Lovisa *et al.* 2015) stated that

EMT program of tubular epithelial cells (TECs) causes severe damage and host response, leading to chronic fibrosis.

On Transmission Electron Microscopy, ultrastructural changes like severe degeneration of alveolar epithelial cells with loss of mitochondria as vacuolations and collagen deposition around the alveolar epithelial cells in BLM challenged mice were alleviated by SAB resulting in restoration of mitochondrial damage in alveolar epithelial cells and decreased collagen deposition was observed. Due to the anti-oxidant effect, SAB might have maintained redox homeostasis and this homeostasis is very closely associated with mitochondrial morphology and its function (Willems *et al.* 2015). This anti-oxidant effect might have been either by the reduction in the level of ROS and 8-hydroxy-2-deoxy Guanosine (8-OHdG) production or SAB might have alleviated the production of Glutathione and Lipid peroxidation which in turn might have suppressed the superoxide generation from mitochondria via a vis mitochondrial depolarization and apoptosis in bronchial epithelial cells in a dose dependent manner. In addition to this, SAB could have significantly up-regulated/ induced overexpression of mortalin (an important mitochondrial chaperone) protein levels inhibiting cell apoptosis by attenuating/ reducing accumulation of ROS (Liu *et al.* 2005, Qu *et al.* 2011) and led to maintenance of mitochondrial homeostasis (Kaul *et al.* 2002, Wadhwa *et al.* 2002).

In conclusion, Salvianolic acid B is effective in alleviating the BLM induced lung fibrosis through suppression of oxidative stress, inflammation, histological, ultrastructural changes and EMT. This study provides an additional knowledge on the ameliorative effect of SAB on BLM induced lung pathology and this may help in the therapeutic or management of pulmonary fibrosis.

Acknowledgements

The author acknowledged the financial support provided by Science and Engineering Research Board (SERB), Department of Science and Technology, Government of India via project No. YSS/2014/000045. We also acknowledge the help provided by Dr. Nitika Thakur and Dr. Asiya Lone and by Sophisticated Analytical Instrument Facility, All India Institute of Medical Sciences, New Delhi for transmission electron microscopy.

References

- Borzone G., Moreno R., Urrea R., Meneses M., Oyarzún M. & Lisboa C. 2001. Bleomycin-induced chronic lung damage does not resemble human idiopathic pulmonary fibrosis. *Am J Respir Crit Care Med*, **163** (7), 1648-1653.
- Chen F., Wang C., Sun J., Wang J., Wang L. & Li J. 2016. Salvianolic acid B reduced the formation of epidural fibrosis in an experimental rat model. *J Orthop Surg Res*, **11**, 141.
- Chen L.J., Ye H., Zhang Q., Li F.Z., Song L.J., Yang J., Mu Q., Rao S.S., Cai P.C., Xiang F., Zhang J.C., Su Y., Xin J.B. & Ma W.L. 2015. Bleomycin induced epithelial-mesenchymal transition (EMT) in pleural mesothelial cells. *Toxicol Appl Pharmacol*, **283** (2), 75-82.
- Cheng D.S., Han W., Chen S.M., Sherrill T.P., Chont M., Park G.Y., Sheller J.R., Polosukhin V.V., Christman J.W., Yull F.E. & Blackwell T.S. 2007. Airway epithelium controls lung inflammation and injury through the NF-kappa B pathway. *J Immunol*, **178** (10), 6504-6513.
- Cheng F., Shen Y., Mohanasundaram P., Lindström M., Ivaska J., Ny T. & Eriksson J.E. 2016. Vimentin coordinates fibroblast proliferation and keratinocyte differentiation in wound healing via TGF-β-Slug signaling. *Proc Natl Acad Sci USA*, **113** (30), E4320-E4327.
- Choi J., Park S.Y. & Joo C.K. 2007. Transforming growth factor-beta1 represses E-cadherin production via slug expression in lens epithelial cells. *Invest Ophthalmol Vis Sci*, **48**, 2708-2718.
- Dejana E., Orsenigo F. & Lampugnani M.G. 2008. The role of adherens junctions and VE-cadherin in the control of vascular permeability. *J Cell Sci*, **121** (Pt 13), 2115-2122.
- Desmoulière A. 1995. Factors influencing myofibroblast differentiation during wound healing and fibrosis. *Cell Biol Int*, **19** (5), 471-476.
- Grande M.T., Sánchez-Laorden B., López-Blau C., De Frutos C.A., Boutet A., Arévalo M., Rowe R.G., Weiss S.J., López-Novoa J.M. & Nieto M.A. 2015. Snail1-induced partial epithelial-to-mesenchymal transition drives renal fibrosis in mice and can be targeted to reverse established disease. *Nat Med*, **21** (9), 989-997.
- Izbicki G., Segel M.J., Christensen T.G., Conner M.W. & Breuer R. 2002. Time course of bleomycin-induced lung fibrosis. *Int J Exp Pathol*, **83** (3), 111-119.
- Jinde K., Nikolic-Paterson D.J., Huang X.R., Sakai H., Kurokawa K., Atkins R.C. & Lan H.Y. 2001. Tubular phenotypic change in progressive tubulointerstitial fibrosis in human glomerulonephritis. *Am J Kidney Dis*, **38** (4), 761-769.
- Kagalwalla A.F., Akhtar N., Woodruff S.A., Rea B.A., Masterson J.C., Mukkada V., Parashette K.R., Du J., Fillon S., Protheroe C.A., Lee J.J., Amsden K., Melin-Aldana H., Capocelli K.E., Furuta G.T. & Ackerman S.J. 2012. Eosinophilic esophagitis: epithelial mesenchymal transition contributes to esophageal remodeling and reverses with treatment. *J Allergy Clin Immunol*, **129**, 1387-1396.
- Kaul S.C., Taira K., Pereira-Smith O.M. & Wadhwa R. 2002. Mortalin: present and prospective. *Exp Gerontol*, **37** (10-11), 1157-1164.
- Leishangthem G.D., Mabalirajan U., Singh V.P., Agrawal A., Ghosh B. & Dinda A.K. 2013. Ultrastructural changes of airway in murine models of allergy and diet-induced metabolic syndrome. *ISRN Allergy*, 261297. doi: 10.1155/2013/261297
- Liu B., Cao B., Zhang D., Xiao N., Chen H., Li G.Q., Peng S.C. & Wei L.Q. 2016. Salvianolic acid B protects against paraquat-induced pulmonary injury by mediating Nrf2/Nox4 redox balance and TGF-β1/Smad3 signaling. *Toxicol Appl Pharmacol*, **309**, 111-120.
- Liu M., Zheng M., Xu H., Liu L., Li Y., Xiao W., Li J. & Ma E. 2015. Anti-pulmonary fibrotic activity of salvianolic acid B was screened by a novel method based on the cyto-biophysical properties. *Biochem Biophys Res Commun*, **468** (1-2), 214-220.
- Liu Q., Chu H., Ma Y., Wu T., Qian F., Ren X., Tu W., Zhou X., Li Jin., Wu W. & Wang J. 2016. Salvianolic acid B attenuates experimental pulmonary fibrosis through inhibition of the TGF-β signaling pathway. *Sci Rep*, **6**, 27610.
- Liu Y., Liu W., Song X.D. & Zuo J. 2005. Effect of GRP75/mthsp70/PBP74/mortalin overexpression on intracellular ATP level, mitochondrial membrane potential and ROS accumulation following glucose deprivation in PC12 cells. *Mol Cell Biochem*, **268** (1-2), 45-51.
- Lomas N.J., Watts K.L., Akram K.M., Forsyth N.R. & Spiteri M.A. 2012. Idiopathic pulmonary fibrosis: immunohistochemical analysis provides fresh insights into lung tissue remodelling with implications for novel prognostic markers. *Int J Clin Exp Pathol*, **5**, 58-71.
- Lovisa S., LeBleu V.S., Tampe B., Sugimoto H., Vadrnagara K., Carstens J.L., Wu C.C., Hagos Y., Burckhardt B.C., Pentcheva-Hoang T., Nischal H., Allison J.P., Zeisberg M. & Kalluri R. 2015. Epithelial-to-mesenchymal transition induces cell cycle arrest and parenchymal damage in renal fibrosis. *Nat Med*, **21** (9), 998-1009.
- Mabalirajan U., Ahmad T., Leishangthem G.D., Joseph D.A., Dinda A.K., Agrawal A. & Ghosh B. 2010. Beneficial effects of high dose of L-arginine on airway hyperresponsiveness and airway inflammation in a murine model of asthma. *J Allergy Clin Immunol*, **125**, 626-635.
- Maretta M., Toth S., Joncová Z., Kruzliak P., Kubatka P., Pingorova S. & Vesela J. 2014. Immunohistochemical expression of MPO, CD163 and VEGF in inflammatory cells in acute respiratory distress syndrome: a case report. *Int J Clin Exp Pathol*, **7** (7), 4539-4544.
- Martin W.J. & Kachel D.L. 1987. Bleomycin-induced pulmonary endothelial cell injury: evidence for the role of iron-catalyzed toxic oxygen-derived species. *J Lab Clin Med*, **110**, 153-158.
- Moeller A., Ask K., Warburton D., Gaudie J. & Kolb M. 2008. The bleomycin animal model: a useful tool to investigate treatment options for idiopathic pulmonary fibrosis. *Int J Biochem Cell Biol*, **40**, 362-382.

- Nishitani Y., Iwano M., Yamaguchi Y., Harada K., Nakatani K., Akai Y., Nishino T., Shiiki H., Kanauchi M., Saito Y. & Neilson E.G. 2005. Fibroblast-specific protein 1 is a specific prognostic marker for renal survival in patients with IgAN. *Kidney Int*, **68** (3), 1078-1085.
- Oikonomou N., Harokopos V., Zalevsky J., Valavanis C. & Kotanidou A. 2006. Soluble TNF mediates the transition from pulmonary inflammation to fibrosis. *PLoS ONE*, **1** (1), e108.
- Qu M., Zhou Z., Xu S., Chen C., Yu Z. & Wang D. 2011. Mortalin overexpression attenuates beta-amyloid-induced neurotoxicity in SH-SY5Y cells. *Brain Res*, **1368**, 336-345.
- Rafii R., Juarez M.M., Albertson T.E. & Chan A.L. 2013. A review of current and novel therapies for idiopathic pulmonary fibrosis. *J Thorac Dis*, **5**, 48-73.
- Rastaldi M.P., Ferrario F., Giardino L., Dell'Antonio G., Grillo C., Grillo P., Strutz F., Müller G.A., Colasanti G. & D'Amico G. 2002. Epithelial-mesenchymal transition of tubular epithelial cells in human renal biopsies. *Kidney Int*, **62** (1), 137-146.
- Ricciardolo F.L., Sterk P.J., Gaston B. & Folkerts G. 2004. Nitric oxide in health and disease of the respiratory system. *Physiol Rev*, **84** (3), 731-765.
- Rosenbloom J., Macarak E., Piera-Velazquez S., Jimenez S.A. 2017. Human fibrotic diseases: current challenges in fibrosis research. *Methods Mol Biol*, **1627**, 1-23.
- Saito F., Tasaka S., Inoue K., Miyamoto K., Nakano Y., Ogawa Y., Yamada W., Shiraishi Y., Hasegawa N., Fujishima S., Takano H. & Ishizaka A. 2008. Role of interleukin-6 in bleomycin-induced lung inflammatory changes in mice. *Am J Respir Cell Mol Biol*, **38**, 566-571.
- Shafiq-ur-Rehman S. 1984. Lead-induced regional lipid peroxidation in brain. *Toxicol Lett*, **21**, 333-337.
- Singh N.D., Sharma A.K., Dwivedi P., Leishangthem G.D., Rahman S., Reddy J. & Kumar M. 2013. Effect of feeding graded doses of citrinin on apoptosis and oxidative stress in male Wistar rats through the F1 generation. *Toxicol Ind Health*, **32**, 385-397.
- Sugiura H. & Ichinose M. 2011. Nitrate stress in inflammatory lung diseases. *Nitric Oxide*, **25** (2), 138-144.
- Tatler A.L. & Jenkins G. 2012. TGF- β activation and lung fibrosis. *Proc Am Thorac Soc*, **9** (3), 130-136.
- Todd N.W., Luzina I.G. & Atamas S.P. 2012. Molecular and cellular mechanisms of pulmonary fibrosis. *Fibrogenesis Tissue Repair*, **5** (1), 11.
- Wadhwa R., Taira K. & Sunil C.K. 2002. An Hsp70 family chaperone, mortalin/mthsp70/PBP74/Grp75: what, when, and where? *Cell Stress Chaperones*, **7** (3), 309-316.
- Wang S.X., Hu L.M., Gao X.M., Guo H. & Fan G.W. 2010. Anti-inflammatory activity of salvianolic acid B in microglia contributes to its neuroprotective effect. *Neurochem Res*, **35** (7), 1029-1037.
- Ware L.B. & Matthay M.A. 2000. The acute respiratory distress syndrome. *N Engl J Med*, **342** (18), 1334-1349.
- Willems P.H., Rossignol R., Dieteren C.E., Murphy M.P. & Koopman W.J. 2015. Redox homeostasis and mitochondrial dynamics. *Cell Metab*, **22** (2), 207-218.
- Willis B.C. & Borok Z. 2007. TGF-beta-induced EMT: mechanisms and implications for fibrotic lung disease. *Am J Physiol Lung Cell Mol Physiol*, **293** (3), L525-L534.
- Wu Y.J., Hong C.Y., Lin S.J., Wu P. & Shiao M.S. 1998. Increase of vitamin E content in LDL and reduction of atherosclerosis in cholesterol-fed rabbits by a water-soluble antioxidant-rich fraction of *Salvia miltiorrhiza*. *Arterioscler Thromb Vasc Biol*, **18** (3), 481-486.
- Xia Z.B., Yuan Y.J., Zhang Q.H., Li H., Dai J.L. & Min J.K. 2018. Salvianolic Acid B suppresses inflammatory mediator levels by downregulating NF- κ B in a rat model of rheumatoid arthritis. *Med Sci Monit*, **24**, 2524-2532.
- Yang C.W., Liu H., Li X.D., Sui S.G. & Liu Y.F. 2018. Salvianolic acid B protects against acute lung injury by decreasing TRPM6 and TRPM7 expressions in a rat model of sepsis. *J Cell Biochem*, **119** (1), 701-711.
- Yang L., Hu J., Hao H.Z., Yin Z., Liu G. & Zou X.J. 2015. Sodium tanshinone IIA sulfonate attenuates the transforming growth factor- β 1-induced differentiation of atrial fibroblasts into myofibroblasts *in vitro*. *Int J Mol Med*, **35**, 1026-1032.